



# Thermal properties and thermodynamic model of lithium doped 45S5 bioglass

Mária Chromčíková<sup>1,2,3</sup> · Branislav Hruška<sup>2,3</sup> · Aleksandra Nowicka<sup>2,3</sup> · Jan Macháček<sup>3</sup> · Marek Liška<sup>1,2,3</sup>

Received: 19 July 2023 / Accepted: 12 October 2023  
© The Author(s) 2023

## Abstract

Shakhmatkin and Vedishcheva thermodynamic model (SV TDM) of the 45S5 Bioglass® doped with three different amounts of Li<sub>2</sub>O (4.1, 9.9, and 12.3 mol%) was evaluated at T = 800 K. The 55 components of SV TDM were considered, among them 12 lithium containing compounds. Different number of components with not negligible equilibrium molar amount was found for different glass compositions (9 or 10). In all glass compositions containing nonzero amount of Li<sub>2</sub>O, the four lithium compounds with not negligible equilibrium amount were identified, i.e., Li<sub>2</sub>O·SiO<sub>2</sub>, 3Li<sub>2</sub>O·P<sub>2</sub>O<sub>5</sub>, Li<sub>2</sub>O·2CaO·2SiO<sub>2</sub>, and 2Li<sub>2</sub>O·SiO<sub>2</sub>. In the 45S5 glass composition four phosphate compounds with not negligible abundance were identified: 9Na<sub>2</sub>O·6SiO<sub>2</sub>·2P<sub>2</sub>O<sub>5</sub>, Na<sub>2</sub>O·2CaO·P<sub>2</sub>O<sub>5</sub>, 5Na<sub>2</sub>O·4SiO<sub>2</sub>·P<sub>2</sub>O<sub>5</sub>, and Na<sub>2</sub>O·CaO·P<sub>2</sub>O<sub>5</sub>. In all other glasses the 3Li<sub>2</sub>O·P<sub>2</sub>O<sub>5</sub> was found with not negligible abundance. Moreover, in the glass with 4.1 mol% Li<sub>2</sub>O the Na<sub>2</sub>O·2CaO·P<sub>2</sub>O<sub>5</sub> and 3Li<sub>2</sub>O·P<sub>2</sub>O<sub>5</sub> compounds were found with not negligible abundance. For each studied glass the glass transition temperature, coefficient of thermal expansion of glass and metastable melt were measured by thermodilatometry. The low temperature viscosity was measured by thermomechanical analysis. The viscous flow activation energy was evaluated from the viscosity temperature dependence. The compositional dependence of measured thermal properties was analyzed by correlation analysis with the Q-distribution of silicate and phosphate units.

**Keywords** 45S5 bioglass · Li<sub>2</sub>O · Thermodynamic model · TMA

## Introduction

One of the most successful glassy materials in the field of biomedicine is the Bioglass® denoted 45S5. This glass has the following composition: 45 mass% SiO<sub>2</sub> (hence the denotation “45S”), 24.5 mass% CaO, 24.5 mass% Na<sub>2</sub>O and 6 mass% P<sub>2</sub>O<sub>5</sub>. The high Ca:P ratio favors the formation of apatite crystals, where the silicon and calcium atoms can act as crystallization centers. At the same time, this ratio (which

is close to that of the actual bone matter) ensures that the human body will accept this artificial material without a negative immune response. Typical utilization of the Bioglass® 45S5 involves bone transplants, maxillofacial, and dental replacements, or stimulation of vessel/nerve regeneration [1–6]. The functionality of the Bioglass® particles is based on the formation of the surface coat of silica gel supporting (at contact with the body fluid) the adhesion of PO<sub>4</sub><sup>3-</sup>, CO<sub>3</sub><sup>2-</sup> and Ca<sup>2+</sup> ions, creating a porous layer of hydroxyapatite. Such surface is then colonized by the stem cells, producing osteocytes and osteoblasts. The osteoblasts then secrete mineral precursors (calcium and phosphate rich structures containing organic material, such as acidic proteins) that consequently form the bone tissue [4–10]. The Bioglass® can be doped by large variety of elements, influencing its bioactivity, mechanical and biological response:

Zn—antibacterial, antifungal and anti-inflammatory effects [11–13];

Sr—supports bone regeneration [14, 15];

✉ Mária Chromčíková  
maria.chromcikova@tuni.sk

<sup>1</sup> Vitrum Laugaricio – Joint Glass Center of IIC SAS, TnU AD, and FChPT STU, Študentská 2, 911 50 Trenčín, Slovak Republic

<sup>2</sup> FunGlass – Centre for Functional and Surface Functionalized Glass, A. Dubček University of Trenčín, Študentská 2, 911 50 Trenčín, Slovak Republic

<sup>3</sup> Department of Glass and Ceramics, Faculty of Chemical Technology, University of Chemistry and Technology, Technická 5, 166 28 Prague, Czech Republic

**Table 1** Composition of the studied Li-doped bioactive glasses and the 45S5 Bioglass® in mol%

Oxide	Glass abbreviation			
	Li0	Li1	Li2	Li3
SiO <sub>2</sub>	47.5	45.6	43.9	41.8
CaO	27.6	26.3	25.2	23.8
Na <sub>2</sub> O	22.3	21.9	19.8	20.0
P <sub>2</sub> O <sub>5</sub>	2.6	2.1	1.2	2.0
Li <sub>2</sub> O	0.0	4.1	9.9	12.3

Ce—exhibits anti-inflammatory and antibacterial properties and supports osteogenesis (bone development) [16–19];

Ga—promotes osteogenesis and exhibits antibacterial activity [20, 21].

One of the very important dopants are the Li<sup>+</sup> ions. Substitution of the sodium ions by the lithium ones has markedly positive effect on the growth rate of the cell cultures, as well as on the activity of the alkaline phosphatase [22, 23]. Formation of the higher density bone tissue was reported [24–26] because of the cultivation on the Li-doped the Bioglass®. Similarly, positive influence of Li-incorporation on the bioactivity of the 45S5 Bioglass® was reported in [27, 28]. The confirmation of the enhanced bioactivity of the Li-doped the Bioglass® is, however, only half the picture needed for the successful application of these materials. The physico-chemical properties of the glasses are just as important, as they determine their workability, long-term stability, and processing conditions. Surprisingly, no available literature sources on the glass transition kinetics and the structural relaxation phenomena in the Li-doped the Bioglass® 45S5 have been found by the authors. Therefore, this work is aimed to investigate the above-mentioned features of the Li-doped bioactive glasses. In the work of the authors Khorami et al. [27] reported the incorporation of Li<sup>+</sup> into bioactive glasses, who focused on the modification of Na<sub>2</sub>O with different amounts of Li<sub>2</sub>O (3, 7 and 12 wt%) in the Bioglass® 45S5 glass system. Many other studies focused on investigating the effect of adding Li<sup>+</sup> to various biomaterials to investigate the osteogenic potential [26–31], but not on the evaluation of physicochemical and structural properties.

When studying the relationships between the structure, composition and properties of glasses, the method of thermodynamic modeling is intensively used, e.g.

Conrad et al., Liška et al., Vedishcheva et al., Pedone et al., Bhaskar et al. [32–37].

This work deals with the application of the Shakhmatkin and Vedishcheva thermodynamic model (SV TDM) for the 45S5 Bioglass® doped with three different amounts of Li<sub>2</sub>O (4.1, 9.9, and 12.3 mol%). SV TDM was evaluated at  $T=800$  K roughly corresponding to the glass transition temperature ( $T_g$ ). For each studied glass the glass transition temperature, coefficient of thermal expansion of glass ( $\alpha_g$ ) and metastable melt ( $\alpha_m$ ) were measured by dilatometry. The low temperature viscosity was measured by thermomechanical analysis. The activation energy of the viscous flow was evaluated from the measured temperature dependence of viscosity. The compositional dependence of the measured thermal properties was analyzed using correlation analysis with the Q-distribution of silicate and phosphate units.

## Experimental part

The 45S5 Bioglass® and doped the bioactive glass were prepared by mixing raw materials of analytical purity ( $\geq 99\%$ ): SiO<sub>2</sub> (Centralchem, Slovakia), CaCO<sub>3</sub> (Centralchem, Slovakia) Na<sub>2</sub>CO<sub>3</sub> (Penta, Czech Republic), Li<sub>2</sub>CO<sub>3</sub> (Penta, Czech Republic), and Na<sub>5</sub>P<sub>3</sub>O<sub>10</sub> (Sigma-Aldrich, Slovakia) and subsequent homogenization for 6 h.

The mixture was then melted in an ambient atmosphere in a Pt-10% Rh crucible in a superkanthal furnace at temperatures in the range of 1300–1400 °C for two hours. During melting, sufficient homogeneity of the melt was ensured by manually stirring. After the melt was clarified, the melting process ended and the clear glass was poured onto a stainless plate, which was then placed in a cooling furnace. The cooling process consisted of tempering at a temperature of 550 °C for 30 min and controlled cooling at 5 °C/min. to laboratory temperature.

The amorphous nature of the glasses was confirmed using the X-ray diffractometer Panalytical Empyrean DY1098—XRD.

The chemical composition of the prepared glasses was determined by the XRF analyzer S8 Tiger (Bruker). The glasses were ground in an agate ball mill to a powder with a

**Table 2** Measured thermal properties of studied glasses

	$10^6\alpha_g/^\circ\text{C}^{-1}$	$10^6\alpha_m/^\circ\text{C}^{-1}$	$T_g/^\circ\text{C}$	A	B/K	$s_{\text{apr}}/\log(\eta/\text{dPa s}^{-1})$	$E_{\eta^*}/\text{kJ mol}^{-1}$
Li0	15.92 ± 0.02	44.68 ± 0.39	475 ± 0.8	−27.6 ± 1.1	32 222 ± 980	0.12	617 ± 19
Li1	13.29 ± 0.01	52.07 ± 0.42	402 ± 0.9	−27.9 ± 1.3	28 913 ± 986	0.15	554 ± 19
Li2	14.46 ± 0.01	48.23 ± 0.37	450 ± 1.0	−26.3 ± 1.1	29 661 ± 938	0.12	568 ± 18
Li3	15.81 ± 0.02	46.41 ± 0.45	407 ± 0.9	−26.8 ± 0.7	28 205 ± 521	0.06	540 ± 10

**Table 3** Input data of SV TDM (considered components, their Q-units, and molar Gibbs energies  $G_m$ )

No	Abbr	Formula	$-G_m/\text{MJ mol}^{-1}$	$Q^n$
1	N	Na <sub>2</sub> O	0.5034	–
2	C	CaO	0.6078	–
3	P	P <sub>2</sub> O <sub>5</sub>	1.6457	2Q <sub>P</sub> <sup>3</sup>
4	Si	SiO <sub>2</sub>	0.9671	Q <sub>Si</sub> <sup>4</sup>
5	Li	Li <sub>2</sub> O	6.4775	–
6	NS2	Na <sub>2</sub> O·2SiO <sub>2</sub>	2.6698	2Q <sub>Si</sub> <sup>3</sup>
7	NS	Na <sub>2</sub> O·SiO <sub>2</sub>	1.6985	Q <sub>Si</sub> <sup>2</sup>
8	N3S2	3Na <sub>2</sub> O·2SiO <sub>2</sub>	4.0146	2Q <sub>Si</sub> <sup>1</sup>
9	N2S	2Na <sub>2</sub> O·SiO <sub>2</sub>	2.3218	Q <sub>Si</sub> <sup>0</sup>
10	N3S8	3Na <sub>2</sub> O·8SiO <sub>2</sub>	9.8947	2Q <sub>Si</sub> <sup>4</sup> + 6Q <sub>Si</sub> <sup>3</sup>
11	N5S	5Na <sub>2</sub> O·SiO <sub>2</sub>	3.7828	Q <sub>Si</sub> <sup>0</sup>
12	C2S	2CaO·SiO <sub>2</sub>	2.4449	Q <sub>Si</sub> <sup>0</sup>
13	C3S2	3CaO·2SiO <sub>2</sub>	4.1846	2Q <sub>Si</sub> <sup>1</sup>
14	CS	CaO·SiO <sub>2</sub>	1.7375	Q <sub>Si</sub> <sup>2</sup>
15	C3S	3CaO·SiO <sub>2</sub>	3.1089	Q <sub>Si</sub> <sup>0</sup>
16	CS2	CaO·2SiO <sub>2</sub>	2.7098	2Q <sub>Si</sub> <sup>3</sup>
17	NP	Na <sub>2</sub> O·P <sub>2</sub> O <sub>5</sub>	2.6907	2Q <sub>P</sub> <sup>2</sup>
18	N5P3	5Na <sub>2</sub> O·3P <sub>2</sub> O <sub>5</sub>	9.8017	2Q <sub>P</sub> <sup>2</sup> + 4Q <sub>P</sub> <sup>1</sup>
19	N2P	2Na <sub>2</sub> O·P <sub>2</sub> O <sub>5</sub>	3.5520	2Q <sub>P</sub> <sup>1</sup>
20	N3P	3Na <sub>2</sub> O·P <sub>2</sub> O <sub>5</sub>	4.2283	2Q <sub>P</sub> <sup>0</sup>
21	CP	CaO·P <sub>2</sub> O <sub>5</sub>	2.6754	2Q <sub>P</sub> <sup>2</sup>
22	C2P	2CaO·P <sub>2</sub> O <sub>5</sub>	3.5517	2Q <sub>P</sub> <sup>1</sup>
23	C3P	3CaO·P <sub>2</sub> O <sub>5</sub>	4.3811	2Q <sub>P</sub> <sup>0</sup>
24	C2P3	2CaO·3P <sub>2</sub> O <sub>5</sub>	6.9744	2Q <sub>P</sub> <sup>3</sup> + 4Q <sub>P</sub> <sup>2</sup>
25	C4P	4CaO·P <sub>2</sub> O <sub>5</sub>	5.0608	2Q <sub>P</sub> <sup>0</sup>
26	C4P3	4CaO·3P <sub>2</sub> O <sub>5</sub>	8.8234	4Q <sub>P</sub> <sup>2</sup> + 2Q <sub>P</sub> <sup>1</sup>
27	CP2	CaO·2P <sub>2</sub> O <sub>5</sub>	4.3396	2Q <sub>P</sub> <sup>3</sup> + 2Q <sub>P</sub> <sup>2</sup>
28	PS	P <sub>2</sub> O <sub>5</sub> ·SiO <sub>2</sub>	2.6762	Q <sub>Si</sub> <sup>4</sup> + 2Q <sub>P</sub> <sup>3</sup>
29	P2S3	2P <sub>2</sub> O <sub>5</sub> ·3SiO <sub>2</sub>	6.3038	3Q <sub>Si</sub> <sup>4</sup> + 4Q <sub>P</sub> <sup>3</sup>
30	NC2S2	Na <sub>2</sub> O·2CaO·2SiO <sub>2</sub>	4.1211	Q <sub>Si</sub> <sup>1</sup>
31	NC3S3	Na <sub>2</sub> O·3CaO·3SiO <sub>2</sub>	5.2135	3Q <sub>Si</sub> <sup>2</sup>
32	NC3S6	Na <sub>2</sub> O·3CaO·6SiO <sub>2</sub>	8.9239	4Q <sub>Si</sub> <sup>3</sup> + 2Q <sub>Si</sub> <sup>2</sup>
33	NCS5	Na <sub>2</sub> O·CaO·5SiO <sub>2</sub>	6.3490	Q <sub>Si</sub> <sup>4</sup> + 4Q <sub>Si</sub> <sup>3</sup>
34	N2CS3	2Na <sub>2</sub> O·CaO·3SiO <sub>2</sub>	5.1228	3Q <sub>Si</sub> <sup>2</sup>
35	N4C3S5	4Na <sub>2</sub> O·3CaO·5SiO <sub>2</sub>	9.9194	Q <sub>Si</sub> <sup>2</sup> + 4Q <sub>Si</sub> <sup>1</sup>
36	NC2P	Na <sub>2</sub> O·2CaO·P <sub>2</sub> O <sub>5</sub>	4.3670	Q <sub>P</sub> <sup>0</sup>
37	NCP	Na <sub>2</sub> O·CaO·P <sub>2</sub> O <sub>5</sub>	3.6222	2Q <sub>P</sub> <sup>1</sup>
38	N2CP3	2Na <sub>2</sub> O·CaO·3P <sub>2</sub> O <sub>5</sub>	8.1580	6Q <sub>P</sub> <sup>2</sup>
39	NC2P3	Na <sub>2</sub> O·2CaO·3P <sub>2</sub> O <sub>5</sub>	8.1180	6Q <sub>P</sub> <sup>2</sup>
40	N9S6P2	9Na <sub>2</sub> O·6SiO <sub>2</sub> ·2P <sub>2</sub> O <sub>5</sub>	16.6773	6Q <sub>Si</sub> <sup>2</sup> + 4Q <sub>P</sub> <sup>0</sup>
41	N5S4P	5Na <sub>2</sub> O·4SiO <sub>2</sub> ·P <sub>2</sub> O <sub>5</sub>	9.6782	4Q <sub>Si</sub> <sup>2</sup> + 2Q <sub>P</sub> <sup>2</sup>
42	C5PS	5CaO·P <sub>2</sub> O <sub>5</sub> ·SiO <sub>2</sub>	6.8100	Q <sub>Si</sub> <sup>0</sup> + 2Q <sub>P</sub> <sup>0</sup>
43	C7PS2	7CaO·P <sub>2</sub> O <sub>5</sub> ·2SiO <sub>2</sub>	9.2518	2Q <sub>Si</sub> <sup>0</sup> + 2Q <sub>P</sub> <sup>0</sup>
44	LC2S2	Li <sub>2</sub> O·2CaO·2SiO <sub>2</sub>	4.2064	2Q <sub>Si</sub> <sup>1</sup>
45	LC3S6	Li <sub>2</sub> O·3CaO·6SiO <sub>2</sub>	8.8554	2Q <sub>Si</sub> <sup>2</sup> + 4Q <sub>Si</sub> <sup>3</sup>
46	LC4S4	Li <sub>2</sub> O·4CaO·4SiO <sub>2</sub>	7.6601	4Q <sub>Si</sub> <sup>1</sup>

**Table 3** (continued)

No	Abbr	Formula	$-G_m/\text{MJ mol}^{-1}$	$Q^n$
47	LCS	Li <sub>2</sub> O·CaO·SiO <sub>2</sub>	2.4002	Q <sub>Si</sub> <sup>0</sup>
48	L2S	2Li <sub>2</sub> O·SiO <sub>2</sub>	2.4735	Q <sub>Si</sub> <sup>0</sup>
49	LS2	Li <sub>2</sub> O·2SiO <sub>2</sub>	2.7122	2Q <sub>Si</sub> <sup>3</sup>
50	LS	Li <sub>2</sub> O·SiO <sub>2</sub>	1.7483	Q <sub>Si</sub> <sup>2</sup>
51	L3NS2	3Li <sub>2</sub> O·Na <sub>2</sub> O·2SiO <sub>2</sub>	4.8667	2Q <sub>Si</sub> <sup>0</sup>
52	L3P	3Li <sub>2</sub> O·P <sub>2</sub> O <sub>5</sub>	4.4911	2Q <sub>P</sub> <sup>0</sup>
53	L2P	2Li <sub>2</sub> O·P <sub>2</sub> O <sub>5</sub>	3.6169	2Q <sub>P</sub> <sup>1</sup>
54	L5P3	5Li <sub>2</sub> O·P <sub>2</sub> O <sub>5</sub>	9.8668	4Q <sub>P</sub> <sup>1</sup> + 2Q <sub>P</sub> <sup>2</sup>
55	LP	Li <sub>2</sub> O·P <sub>2</sub> O <sub>5</sub>	2.6853	2Q <sub>P</sub> <sup>2</sup>

size fraction below 45 μm. Table 1 shows the experimental composition of studied glasses in mole percentages.

The glass transition was investigated using thermomechanical analysis using TMA Q EM 402 (TA Instrument) [38]. Prismatic samples were prepared by cutting and grinding to a size of 20 × 5 × 5 mm. Dilatometric curves were measured at a heating and cooling rate of 5 °C min<sup>-1</sup> at a sample load of 5 g. Low-temperature viscosity between 10<sup>8</sup> dPa.s and 10<sup>12</sup> dPa.s was measured by a thermomechanical analyzer (Netzsch, TMA 402) [38].

Shakhmatkin and Vedishcheva proposed a thermodynamic model that was successfully applied to the study of silicate and phosphate glasses [39, 40]. According to this model glasses and melts are ideal solutions formed from products of equilibrium chemical reactions between oxides and from the original un-reacted oxides. The input data for construction of SV TDM consists of the molar Gibbs energies of pure crystalline compounds at particular temperature, and the analytical composition of the particular system. The equilibrium molar amount of each of the systems species is obtained by minimization of the system's Gibbs energy constrained by the overall system composition [41]. It was verified that SV TDM can be used for most multicomponent glasses using the crystalline state data. The available databases of thermodynamic data (e.g. FACT [37, 42]) enable the simple construction of the SV TDM for various multicomponent systems. This approach enabled a direct connection between the glass structure and the balanced representation of individual glass components.

## Results and discussion

The temperature dependence of measured viscosity was described by the Andrade's equation [43, 44]:

$$\log \eta = A + \frac{B}{T} \quad (1)$$

**Table 4** Components of SV TDM with not negligible equilibrium molar amount (for each glass composition the components are ordered with decreasing molar amount  $n_{ox}$ )

Li3		Li2		Li1		Li0	
component	$n_{ox}/mol$	component	$n_{ox}/mol$	component	$n_{ox}/mol$	component	$n_{ox}/mol$
NS	0.3852	NS	0.3776	NS	0.3384	NC3S6	0.3564
C3S2	0.1181	C3S2	0.1278	NC3S6	0.2010	NS	0.2550
LC2S2	0.1138	LC2S2	0.1090	CS	0.1132	CS	0.1011
C2S	0.0956	CS	0.1069	C3S2	0.1117	C3S2	0.0894
CS	0.0912	C2S	0.0876	C2S	0.0633	N9S6P2	0.0686
L3P	0.0758	LS	0.0775	NC2P	0.0340	NC2P	0.0525
LS	0.0747	L3P	0.0449	LC2S2	0.0323	C2S	0.0463
NC3S6	0.0110	NC3S6	0.0403	LS	0.0278	N5S4P	0.0114
NC2S2	0.0108	NC2S2	0.0107	L3P	0.0274	NCP	0.0104
L2S	0.0103			N9S6P2	0.0246		

**Table 5** Si Q-distribution and P Q-distribution of SV TDM

	Si Q-distribution/%					P Q-distribution/%			
	Q <sup>0</sup>	Q <sup>1</sup>	Q <sup>2</sup>	Q <sup>3</sup>	Q <sup>4</sup>	Q <sup>0</sup>	Q <sup>1</sup>	Q <sup>2</sup>	Q <sup>3</sup>
Li0	3.26	8.00	53.47	35.24	0.02	83.39	12.24	4.36	0
Li1	4.71	13.49	62.11	19.67	0.02	88.62	8.14	3.25	0
Li2	7.23	22.91	66.09	3.76	0.01	99.08	0.73	0.18	0
Li3	8.47	23.79	66.62	1.11	0.01	99.42	0.49	0.10	0

**Table 6** Correlation coefficients between Li<sub>2</sub>O content and relative amounts of Si Q-units and P Q-units

	Li <sub>2</sub> O	SiQ <sup>0</sup>	SiQ <sup>1</sup>	SiQ <sup>2</sup>	SiQ <sup>3</sup>	SiQ <sup>4</sup>	PQ <sup>0</sup>	PQ <sup>1</sup>	PQ <sup>2</sup>
Li <sub>2</sub> O	1.00	1.00	0.99	0.94	-0.99	-0.97	0.99	-0.99	-0.98
SiQ <sup>0</sup>	1.00	1.00	0.98	0.92	-0.98	-0.99	0.98	-0.98	-0.98
SiQ <sup>1</sup>	0.99	0.98	1.00	0.95	-0.99	-0.96	1.00	-1.00	-1.00
SiQ <sup>2</sup>	0.94	0.92	0.95	1.00	-0.98	-0.84	0.94	-0.95	-0.92
SiQ <sup>3</sup>	-0.99	-0.98	-0.99	-0.98	1.00	0.93	-0.99	0.99	0.98
SiQ <sup>4</sup>	-0.97	-0.99	-0.96	-0.84	0.93	1.00	-0.95	0.95	0.96
PQ <sup>0</sup>	0.99	0.98	1.00	0.94	-0.99	-0.95	1.00	-1.00	-1.00
PQ <sup>1</sup>	-0.99	-0.98	-1.00	-0.95	0.99	0.95	-1.00	1.00	1.00
PQ <sup>2</sup>	-0.98	-0.98	-1.00	-0.92	0.98	0.96	-1.00	1.00	1.00

**Table 7** The correlation analysis between the measured properties and Si Q-distribution and P Q-distribution

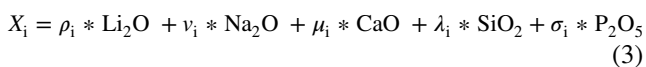
	SiQ <sup>0</sup>	SiQ <sup>1</sup>	SiQ <sup>2</sup>	SiQ <sup>3</sup>	SiQ <sup>4</sup>	PQ <sup>0</sup>	PQ <sup>1</sup>	PQ <sup>2</sup>
$10^6\alpha_g$ [°C <sup>-1</sup> ]	0.11	0.00	-0.28	0.09	-0.28	0.01	0.01	-0.07
$10^6\alpha_m$ [°C <sup>-1</sup> ]	0.01	0.09	0.39	-0.19	0.16	0.07	-0.09	-0.01
$T_g$ [°C]	-0.47	-0.43	-0.64	0.52	0.36	-0.39	0.41	0.35
$E_{\eta^*}$ [kJ.mol <sup>-1</sup> ]	-0.77	-0.76	-0.90	0.82	0.67	-0.73	0.75	0.69

where  $A$ , and  $B$  are constants routinely determined by the regression analysis, and  $T$  is thermodynamic temperature. The activation energy of viscous flow,  $E_{\eta^*}$ , is given by the relation:

$$B = \frac{E_{\eta^*}}{2.303R} \quad (2)$$

where  $R$  is the molar gas constant. The Table 2 summarizes the values of  $A$  and  $B$  calculated by fitting Eq. (1), and the values of activation energy calculated using Eq. (2). The linear thermal expansion coefficients of glass,  $\alpha_g$ , and metastable melt,  $\alpha_m$ , were estimated from the slope of the cooling curve in temperature ranges of 300–350 and 450–550 °C, respectively. The glass transition temperatures,  $T_g$ , were determined from the intersection of two lines with slopes of  $\alpha_g$  and  $\alpha_m$ .

The 55 components of SV TDM were considered (Table 3), among them 12 lithium containing compounds. The significant (not negligible) abundance of system components was defined by the equilibrium molar amount reaching at least 0.01 mol of oxides, i.e.  $n_{\text{ox},i} \geq 0.01$  mol. When the stoichiometry of the  $i$ th component ( $X_i$ ) is expressed by the reaction:



then  $n_{\text{ox},i}$  is defined by:

$$n_{\text{ox},i} = n_i * (\rho_i + v_i + \mu_i + \lambda_i + \sigma_i) \quad (4)$$

where  $n_i$  is the equilibrium molar amount of the  $i$ th component. Different number of components with not negligible equilibrium molar amount was found for different glass compositions (9 or 10), see Table 4. In all glass compositions containing nonzero amount of  $\text{Li}_2\text{O}$ , the four lithium compounds with not negligible equilibrium amount were identified, i.e.  $\text{Li}_2\text{O} \cdot \text{SiO}_2$ ,  $3\text{Li}_2\text{O} \cdot \text{P}_2\text{O}_5$ ,  $\text{Li}_2\text{O} \cdot 2\text{CaO} \cdot 2\text{SiO}_2$ , and  $2\text{Li}_2\text{O} \cdot \text{SiO}_2$ . In the 45S5 glass composition four phosphate compounds with not negligible abundance were identified:  $9\text{Na}_2\text{O} \cdot 6\text{SiO}_2 \cdot 2\text{P}_2\text{O}_5$ ,  $\text{Na}_2\text{O} \cdot 2\text{CaO} \cdot \text{P}_2\text{O}_5$ ,  $5\text{Na}_2\text{O} \cdot 4\text{SiO}_2 \cdot \text{P}_2\text{O}_5$ , and  $\text{Na}_2\text{O} \cdot \text{CaO} \cdot \text{P}_2\text{O}_5$ . In all other glasses the  $3\text{Li}_2\text{O} \cdot \text{P}_2\text{O}_5$  was found with not negligible abundance. Moreover, in the glass with 4.1 mol%  $\text{Li}_2\text{O}$  the  $\text{Na}_2\text{O} \cdot 2\text{CaO} \cdot \text{P}_2\text{O}_5$  and  $3\text{Li}_2\text{O} \cdot \text{P}_2\text{O}_5$  compounds were found with not negligible abundance.

Due to volatility of glass components during glass melting the analyzed glass composition strongly differs from the prescribed one. Due to this fact no straightforward dependence of measured quantities on the molar content of lithium oxide was found. On the other hand, some relationships were found by the  $\text{Li}_2\text{O}$  influence on the Si Q-distribution and P Q-distribution (Table 5). First the mutual relationships between Si Q-units and between P Q-units were found. Increase of Li content increases  $\text{SiQ}^0$ ,  $\text{SiQ}^1$ , and  $\text{SiQ}^2$ , and simultaneously decreases the amount of  $\text{SiQ}^3$ , and  $\text{SiQ}^4$ . Similarly, Li content increases  $\text{PQ}^0$  and decreases  $\text{PQ}^1$  and  $\text{PQ}^2$ .

It was found that  $\text{SiQ}^0$ ,  $\text{SiQ}^1$ , and  $\text{SiQ}^2$  are strongly positively correlated (Table 6). Similarly,  $\text{SiQ}^3$ , and  $\text{SiQ}^4$  are strongly positively correlated. The strong positive correlation means that correlated quantities are changed proportionally in the same direction. Thus, decreasing of the content

of  $\text{SiQ}^3$ , and  $\text{SiQ}^4$  (caused by decreasing of the degree of networking) leads to increase of  $\text{SiQ}^0$ ,  $\text{SiQ}^1$ , and  $\text{SiQ}^2$ . Similarly, it is with phosphate Q-units. It was found that  $\text{PQ}^1$  and  $\text{PQ}^2$  are strongly positively correlated, and  $\text{PQ}^0$  is strongly negatively correlated with  $\text{PQ}^1$  and  $\text{PQ}^2$ . Thus, decreasing of the content of  $\text{PQ}^1$ , and  $\text{PQ}^2$  (caused by decreasing of the degree of networking) leads to increase of  $\text{PQ}^0$ .

In the next step the correlation analysis between the measured properties an Si Q-distribution and P Q-distribution was analyzed (Table 7). As can be expected for the viscous flow activation energy and the glass transition temperature the strong negative correlation was found with  $\text{SiQ}^0$ ,  $\text{SiQ}^1$ ,  $\text{SiQ}^2$ , and  $\text{PQ}^0$ . Simultaneously the strong positive correlation was identified for  $\text{SiQ}^3$ ,  $\text{SiQ}^4$ ,  $\text{PQ}^1$ , and  $\text{PQ}^2$ . It confirmed that decreasing the degree of networking decreases the values of  $E_{\eta^*}$ , and  $T_g$ . On the other hand, the correlation analysis of the thermal expansion coefficients does not show strongly significant correlations. But in principle (i.e., according to the signs of correlation coefficients) it confirms that decreasing the degree of networking increases the thermal expansion coefficients.

## Conclusions

According to the presented results of SV TDM the 45S5 Bioglass® doped  $\text{Li}_2\text{O}$  bioactive glass can be considered as a homogeneous mixture of 9, or 10 components were present in significant equilibrium molar amount for each studied glass composition. In all glass compositions containing nonzero amount of  $\text{Li}_2\text{O}$ , the four lithium compounds with not negligible equilibrium amount were identified, i.e.  $\text{Li}_2\text{O} \cdot \text{SiO}_2$ ,  $3\text{Li}_2\text{O} \cdot \text{P}_2\text{O}_5$ ,  $\text{Li}_2\text{O} \cdot 2\text{CaO} \cdot 2\text{SiO}_2$ , and  $2\text{Li}_2\text{O} \cdot \text{SiO}_2$ . In the 45S5 glass composition four phosphate compounds with not negligible abundance were identified:  $9\text{Na}_2\text{O} \cdot 6\text{SiO}_2 \cdot 2\text{P}_2\text{O}_5$ ,  $\text{Na}_2\text{O} \cdot 2\text{CaO} \cdot \text{P}_2\text{O}_5$ ,  $5\text{Na}_2\text{O} \cdot 4\text{SiO}_2 \cdot \text{P}_2\text{O}_5$ , and  $\text{Na}_2\text{O} \cdot \text{CaO} \cdot \text{P}_2\text{O}_5$ . In all other glasses the  $3\text{Li}_2\text{O} \cdot \text{P}_2\text{O}_5$  was found with not negligible abundance. Moreover, in the glass with 4.1 mol%  $\text{Li}_2\text{O}$  the  $\text{Na}_2\text{O} \cdot 2\text{CaO} \cdot \text{P}_2\text{O}_5$  and  $3\text{Li}_2\text{O} \cdot \text{P}_2\text{O}_5$  compounds were found with not negligible abundance. The viscous flow activation energy and the glass transition temperature the strong negative correlation was found with  $\text{SiQ}^0$ ,  $\text{SiQ}^1$ ,  $\text{SiQ}^2$ , and  $\text{PQ}^0$ . Simultaneously the strong positive correlation was identified for  $\text{SiQ}^3$ ,  $\text{SiQ}^4$ ,  $\text{PQ}^1$ , and  $\text{PQ}^2$ . It confirmed that decreasing the degree of networking decreases the values of  $E_{\eta^*}$ , and  $T_g$ .

**Supplementary Information** The online version contains supplementary material available at <https://doi.org/10.1007/s10973-023-12668-2>.

**Acknowledgements** The financial support of this work by the projects Grant No. VEGA 2/0091/20, VEGA 1/0021/23, and APVV-21-0016.

**Funding** Open access funding provided by The Ministry of Education, Science, Research and Sport of the Slovak Republic in cooperation with Centre for Scientific and Technical Information of the Slovak Republic.

**Open Access** This article is licensed under a Creative Commons Attribution 4.0 International License, which permits use, sharing, adaptation, distribution and reproduction in any medium or format, as long as you give appropriate credit to the original author(s) and the source, provide a link to the Creative Commons licence, and indicate if changes were made. The images or other third party material in this article are included in the article's Creative Commons licence, unless indicated otherwise in a credit line to the material. If material is not included in the article's Creative Commons licence and your intended use is not permitted by statutory regulation or exceeds the permitted use, you will need to obtain permission directly from the copyright holder. To view a copy of this licence, visit <http://creativecommons.org/licenses/by/4.0/>.

## References

- Hench LL. The story of bioglass. *J Mater Sci Mater Med*. 2006;17:967–78. <https://doi.org/10.1007/s10856-006-0432-z>.
- Hench LL, Paschall HA. Direct chemical bond of bioactive glass-ceramic materials to bone and muscle. *J Biomed Mater Res*. 1973;7:25–42. <https://doi.org/10.1002/jbm.820070304>.
- Boccaccini AR, Blaker JJ. Bioactive composite materials for tissue engineering scaffolds. *Expert Rev Med Devices*. 2005;2:303–17. <https://doi.org/10.1586/17434440.2.3.303>.
- Jones JR. Review of bioactive glass: from Hench to hybrids. *Acta Biomater*. 2013;9:4457–86. <https://doi.org/10.1016/j.actbio.2012.08.023>. PMID22922331.
- Baino F, Hamzehlou S, Kargozar S. Bioactive glasses, Where are we and where are we going? *J Funct Biomater*. 2018;9(1):1–25. <https://doi.org/10.3390/jfb9010025>.
- Hench LL, Splinter RJ, Allen WC, Greenlee TK. Bonding mechanisms at the interface of ceramic prosthetic materials. *J Biomed Mater Res*. 1971;5(6):117–41. <https://doi.org/10.1002/jbm.820050611>.
- Chen Q, Thompson I, Boccaccini A. 45S5 Bioglass®-derived glass–ceramic scaffolds for bone tissue engineering. *Biomaterials*. 2006;27(11):2414–25. <https://doi.org/10.1016/j.biomaterials.2005.11.025>. PMID16336997.
- Day RM, Boccaccini AR, Shurey S, Roether JA, Forbes A, Hench LL, Gabe SM. Assessment of polyglycolic acid mesh and bioactive glass for soft-tissue engineering scaffolds. *Biomaterials*. 2004;25:5857–66. <https://doi.org/10.1016/j.biomaterials.2004.01.043>.
- Banchet V, Jallot E, Michel J, Wortham L, Laurent-Maquin D, Balossier G. X-ray microanalysis in STEM of short-term physicochemical reactions at bioactive glass particle/biological fluid interface Determination of O/Si atomic ratios. *Surf Interface Anal Int J Devoted Develop Appl Techn Anal Surf Interfa Thin Films*. 2004;36:658–65. <https://doi.org/10.1002/sia.1916>.
- Rahaman M. Bioactive glass in tissue engineering. *Acta Biomater*. 2011;7:2355–73. <https://doi.org/10.1016/j.actbio.2011.03.016>. PMC3085647.PMID21421084.
- Miola M, Cordero-Arias L, Ferlenda G, Cochis A, Virtanen S, Rimondini L, Verné E, Boccaccini AR. Electrophoretic deposition of composite coatings based on alginate matrix/45S5 bioactive glass particles doped with B Zn or Sr. *Surf Coat Technol*. 2021;418:127183. <https://doi.org/10.1016/j.surfcoat.2021.127183>.
- Özarslan AC, Özel C, Okumuş MD, Doğan D, Yücel S. Development, structural and rheological characterization, and in vitro evaluation of the zinc-doped 45S5 bioactive glass–vaseline ointment for potential wound healing applications. *J Mater Res*. 2023;38:1557–72. <https://doi.org/10.1557/s43578-023-00908-y>.
- Anand V, Singh KJ, Kaur K. Evaluation of zinc and magnesium doped 45S5 mesoporous bioactive glass system for the growth of hydroxyl apatite layer. *J Non-Cryst Solids*. 2014;406:88–94. <https://doi.org/10.1016/j.jnoncrysol.2014.09.050>.
- Amudha S, Ramya JR, Arul KT, Deepika A, Sathiamurthi P, Mohana B, Asokan K, Dong CL, Kalkura SN. Enhanced mechanical and biocompatible properties of strontium ions doped mesoporous bioactive glass. *Compos Part B: Eng*. 2020;196:108099. <https://doi.org/10.1016/j.compositesb.2020.108099>.
- Rifane TO, Cordeiro KE, Silvestre FA, Souza MT, Zanotto ED, Araújo-Neto VG, Giannini M, Sauro S, de Paula DM, Feitosa VP. Impact of silanization of different bioactive glasses in simplified adhesives on degree of conversion, dentin bonding and collagen remineralization. *Dent Mater*. 2023;39:217–26. <https://doi.org/10.1016/j.dental.2023.01.005>.
- Nicolini V, Malavasi G, Menabue L, Lusvardi G, Benedetti F, Valeri S, Luches P. Cerium-doped bioactive 45S5 glasses: spectroscopic, redox, bioactivity and biocatalytic properties. *J Mater Sci*. 2017;52:8845–57. <https://doi.org/10.1007/s10853-017-0867-2>.
- Raimondi S, Zambon A, Ranieri R, Fraulini F, Amaretti A, Rossi M, Lusvardi G. Investigation on the antimicrobial properties of cerium-doped bioactive glasses. *J Biomed Mater Res, Part A*. 2022;110:504–8. <https://doi.org/10.1002/jbm.a.37289>.
- Zambon A, Malavasi G, Pallini A, Fraulini F, Lusvardi G. Cerium containing bioactive glasses. *Biomater Sci Eng*. 2021;7:4388–401. <https://doi.org/10.1021/acsbmaterials.1c00414>.
- Chromčíková M, Svoboda R, Hruška B, Pecušová B, Nowicka A. Thermo-kinetic and structural characterization of Ce-doped glasses based on Bioglass 45S5. *Mater Chem Phys*. 2023;304:1–9. <https://doi.org/10.1016/j.matchemphys.2023.127833>.
- Medeiros GS, Oliveira LFM, Ferreira FV, Souza LP, Martin RA, de Oliveira IR, Lopes JH. A perfect pair: Niobium- and gallium-doped ceramic biomaterial enabled by coupled synthesis method with potential application for bone regeneration and cancer-targeted therapy. *J Non-Cryst Solids*. 2023;599:121962. <https://doi.org/10.1016/j.jnoncrysol.2022.121962>.
- Souza L, Ferreira FV, Lopes JH, Camilli JA, Martin RA. Cancer inhibition and in vivo osteointegration and compatibility of gallium-doped bioactive glasses for osteosarcoma applications. *Appl Mater Interfaces*. 2022;14:45156–66. <https://doi.org/10.1021/acsaami.2c12102>.
- Farmani AR, Salmeh MA, Golkar Z, Moeinzadeh A, Ghiasi FF, Amirabad SZ, Shoormeij MH, Mahdavinezhad F, Momeni S, Moradbeygi F, Ai J, Hardy JG, Mostafaei A. Li-doped bioactive ceramics: promising biomaterials for tissue engineering and regenerative medicine. *J Funct Biomater*. 2022;13:162. <https://doi.org/10.3390/jfb13040162>.
- Chromčíková M, Svoboda R, Pecušová B, Hruška B, Hujová M, Nowicka A, Liška M. Effect of lithium doping on the glass transition behavior of the Bioglass 45S5. *J Non-Cryst Solids*. 2022;594:121797. <https://doi.org/10.1016/j.jnoncrysol.2022.121797>.
- Wu C, Chang J. Multifunctional mesoporous bioactive glasses for effective delivery of therapeutic ions and drug/growth factors. *J Control Release*. 2014;193:282–95. <https://doi.org/10.1016/j.jconrel.2014.04.026>.
- Thorfve A, Bergstrand A, Ekström K, Lindahl A, Thomsen P, Larsson A, Tengvall P. Gene expression profiling of peri-implant healing of PLGA-Li+ implants suggests an activated Wnt signaling pathway in vivo. *PLoS ONE*. 2014;9:e102597. <https://doi.org/>

- [10.1371/journal.pone.0102597](https://doi.org/10.1371/journal.pone.0102597). PMID:25047349; PMCID:PMC4105622.
26. Wu Y, Zhu S, Wu C, Lu P, Hu C, Xiong S, Chang J, Heng BC, Xiao Y, Ouyang HW. A bi-lineage conducive scaffold for osteochondral defect regeneration. *Adv Func Mater*. 2014;24:4473–83. <https://doi.org/10.1002/adfm.201304304>.
  27. Khorami M, Hesarakhi S, Behnamghader A, Nazarian H, Shahrabadi S. In Vitro bioactivity and biocompatibility of lithium substituted 45S5 bioglass. *Mater Sci Eng C*. 2011;31:1584–92.
  28. Thorfve A, Lindahl C, Xia W, Igawa K, Lindahl A, Thomsen P, Palmquist A, Tengvall P. Hydroxyapatite coating affects the Wnt signaling pathway during peri-implant healing in vivo. *Acta Biomater*. 2014;10:1451–62. <https://doi.org/10.1016/j.actbio.2013.12.012>.
  29. Han P, Xu M, Chang J, Chakravorty N, Wu C, Xio Y. Lithium release from -tricalcium phosphate inducing cementogenic and osteogenic differentiation of both hPDLCS and hBMSCs. *Biomater Sci*. 2014;2:1230–43. <https://doi.org/10.1039/C4BM00111G>.
  30. Wang X, Zhu S, Jiang X, Li Y, Song D, Hu J. Systemic administration of lithium improves distracted bone regeneration in rats. *Calcif Tissue Int*. 2015;96:534–40. <https://doi.org/10.1007/s00223-015-0004-7>.
  31. Geng D, Wu J, Shao H, Zhu S, Wang Y, Zhang W, Ping Z, Hu X, Zhu X, Xu Y. Pharmaceutical inhibition of glycogen synthetase kinase 3 beta suppresses wear debris-induced osteolysis. *Biomaterials*. 2015;69:12–21. <https://doi.org/10.1016/j.biomaterials.2015.07.061>.
  32. Conrad R. Thermochemistry and structure of oxide glasses. In: *Analysis of the composition and structure of glass and glass ceramics*. Berlin: Springer; 1999.
  33. Conrad R. A simplified procedure to estimate thermodynamic activities in multicomponent oxide melts. *Molten Salt Forums*. 1998;5–6:155.
  34. Conrad R (1999) Predictive modeling of glass corrosion. In: *Proceedings of the 5th ESG conference*, B1–2–B1–10, Czech Glass Society, Praha
  35. Pedone A, Charpentier T, Malavasi G, Menziani MC. New Insights into the atomic structure of 45S5 bioglass by means of solid-state NMR spectroscopy and accurate first-principles simulations. *Chem Mater*. 2010;22:5644–52. <https://doi.org/10.1021/cm102089c>.
  36. Bhaskar P, Kumar R, Maurya Y, et al. Cooling rate effects on the structure of 45S5 bioglass: insights from experiments and simulations. *J Non-Cryst Solids*. 2020;534:119952. <https://doi.org/10.1016/j.jnoncrysol.2020.119952>.
  37. Liška M, Macháček J, Chromčíková M, Svoboda R. Thermodynamic model of CaO–SiO<sub>2</sub> glasses. *Ceram-Silik*. 2020;64:63–7.
  38. Chromčíková M, Lissová M, Mošner P, Rösslerová I, Liška M, Koudelka L. Viscosity and flow activation for viscous energy of PbO-WO<sub>3</sub>-P<sub>2</sub>O<sub>5</sub> glasses. *Phys Chem Glasses: Eur J Glass Sci Technol B*. 2013;54:129–32.
  39. Vedishcheva NM, Shakhmatkin BA, Shultz MM, Wright AC. The thermodynamic modelling of glass properties: a practical proposition. *J Non-Cryst Solids*. 1996;196:239–43.
  40. Vedishcheva NM, Wright AC. Chemical structure of oxide glasses: a concept for establishing structure-property relationships. In: Schmelzer JWP, editor. *Glass: selected properties and crystallization*. Berlin: de Gruyter; 2014. p. 269–99.
  41. Voňka P, Leitner J. Calculation of chemical equilibria in heterogeneous multicomponent systems. *Calphad*. 1995;19:25–36.
  42. <http://www.crct.polym.tl.ca/fact/> (2023). Accessed 24 April 2023.
  43. Eyring H. Viscosity, plasticity, and diffusion as examples of absolute reaction rates. *J Chem Phys*. 1936;4:283.
  44. Andrade EDC. A theory of the viscosity of liquids Part I. The London, Edinburgh, Dublin Philosoph Magaz J Sci. 1934;17:497.

**Publisher's Note** Springer Nature remains neutral with regard to jurisdictional claims in published maps and institutional affiliations.